



**Multi-State Amine Sensing by Electron Transfers in a
BODIPY Probe**

Journal:	<i>Organic & Biomolecular Chemistry</i>
Manuscript ID	OB-ART-11-2019-002466.R1
Article Type:	Paper
Date Submitted by the Author:	09-Dec-2019
Complete List of Authors:	<p>VanDenburgh, Katherine; Indiana University Bloomington, Chemistry Liu, Yun; Indiana University Bloomington, Chemistry; University of Illinois at Urbana-Champaign, Beckman Institute for Advanced Science and Technology Sadhukhan, Tumpa; Indiana University Bloomington, Chemistry Benson, Christopher; Indiana University Bloomington, Chemistry Cox, Natalie; Indiana University Bloomington, Chemistry Erbas-Cakmak, Sundus; Indiana University Bloomington, Chemistry; Konya Food and Agriculture University, Molecular Biology and Genetics Qiao, Bo; Indiana University Bloomington, Chemistry; Massachusetts Institute of Technology Gao, Xinfeng; Indiana University Bloomington, Chemistry Pink, Maren; Indiana University Bloomington, Chemistry Raghavachari, Krishnan; Indiana University Bloomington, Chemistry Flood, Amar; Indiana University Bloomington, Chemistry</p>

Organic and Biomolecular Chemistry

Multi-State Amine Sensing by Electron Transfers in a BODIPY Probe

Katherine L. VanDenburgh,^a Yun Liu,^{a,b} Tumpa Sadhukhan,^a Christopher R. Benson,^a Natalie M. Cox,^a Sundus Erbas-Cakmak,^{a,c} Bo Qiao,^{a,d} Xinfeng Gao,^a Maren Pink,^a Krishnan Raghavachari,^a and Amar H. Flood^{*a}

^a Department of Chemistry, Indiana University, 800 E. Kirkwood Avenue, Bloomington, IN 47405, USA

^b Present address: Beckman Institute for Advanced Science and Technology, University of Illinois at Urbana-Champaign, Urbana, IL 61801, USA

^c Present address: Department of Molecular Biology and Genetics, Konya Food and Agriculture University, Konya, Turkey

^d Present address: Research Laboratory of Electronics, Massachusetts Institute of Technology, Cambridge, MA 02139, USA

Abstract: Amines are ubiquitous in the chemical industry and are present in a wide range of biological processes, motivating the development of amine-sensitive sensors. There are many turn-on amine sensors, however there are no examples of turn-on sensors that utilize the amine's ability to react by single electron transfer (SET). We investigated a new turn-on amine probe with a 4,4-difluoro-4-bora-3a,4a-diaza-*s*-indacene (BODIPY) fluorophore. BODIPY fluorescence is first preprogrammed into an off state by internal photoinduced electron transfer (PET) to an electron-deficient quinolinium ring, resulting in fluorescence quenching. At low concentrations of aliphatic amine (0 to 10 mM), this PET pathway is shut down by external SET from the amine to the photoexcited charge-transfer state of the probe and the fluorescence is turned on. At high concentrations of amine (50 mM to 1 M), we observed collisional quenching of the BODIPY fluorescence. The probe is selective for aliphatic amines over aromatic amines, and aliphatic thiols or alcohols. These three molecular processes modulate the BODIPY fluorescence in a multi-mechanistic way with two of them producing a direct response to amine concentrations. The totality of the three molecular processes produced the first example of a multi-state and dose-responsive amine sensor.

Introduction

Amines are critically important across numerous chemical and biological processes¹⁻² and are potentially toxic pollutants.³⁻⁶ For these reasons, the need to monitor amines motivates the development of complementary molecular sensors.⁷⁻⁸ There are two common mechanisms used for amine sensing. The first relies on the reactivity of the nitrogen as a nucleophile, i.e., chemidosimeter sensing.⁹⁻¹⁶ For example, the reaction of electron-rich amines, e.g., ethylamine, with 1,3-dimethylbarbiturate displaces a covalently-linked fluorophore to turn on its fluorescence.¹⁴ The second common sensing mechanism utilizes the reactivity of amines as sacrificial electron donors, resulting in turn-off fluorescent sensors.¹⁷⁻²⁷ For example, collisional quenching of perylene diimide fluorescence has been observed with a range of organic amines like aniline and triethylamine across 0.1 to 1 M concentrations in tetrahydrofuran.²² An unexplored area in amine sensing is the use of the electron transfer to generate an irreversible turn-on response with a probe.

When designing molecular sensors, turn-on fluorescent responses (Figure 1a) are preferred. They are less prone to false positives and are easier to detect with the naked eye.²⁸ However, they are also much rarer. To date, there are no examples of amine sensors with a turn-on response that utilize electron transfer from the nitrogen's lone pair. To the best of our knowledge, the closest examples²⁹⁻³³ utilize metallo-macromolecules, such as polymers²⁹⁻³² and metal-organic frameworks,³³ where the turn-on response results from metal coordination from the amine's lone pair. For example, a poly(9,9-dioctylfluorene) polymer was quenched upon incorporation of a palladium porphyrin; the fluorene polymer's fluorescence was restored when amines coordinate to the palladium to prevent the quenching.^{29, 31} Fundamentally, these systems did not use electron transfer to generate the turn-on response.

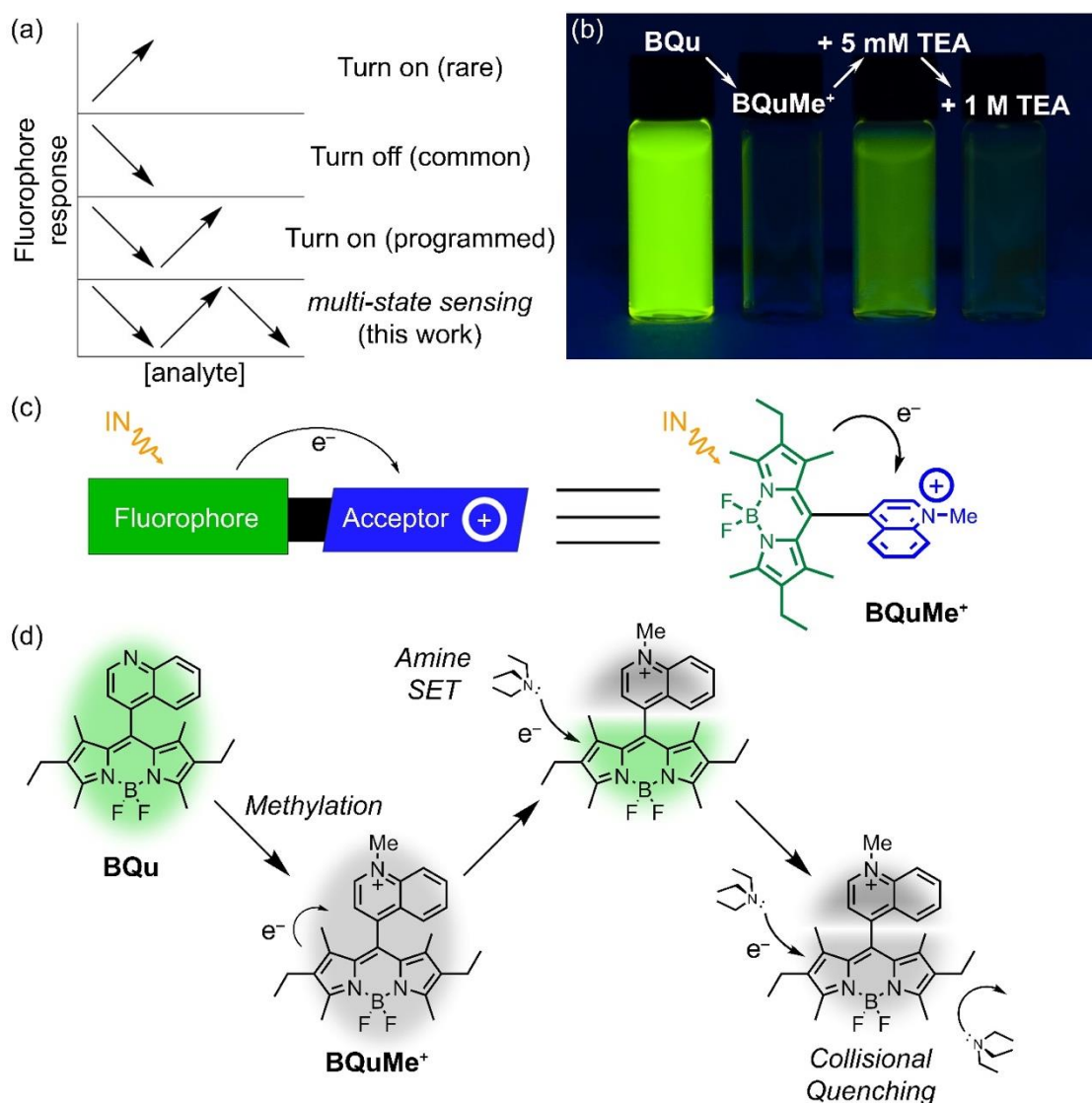


Figure 1. (a) Changes in fluorescence intensity for various sensing mechanisms and the multi-state mechanism described in this work. (b) Black-light photograph of the multi-state sensing mechanism with **BQu** (10 μ M), **BQuMe⁺** (10 μ M), **BQuMe⁺** (10 μ M) with 5 mM of triethylamine, and **BQuMe⁺** (10 μ M) with 1 M of triethylamine (MeCN) (c) General cartoon and the structural representation of the probe, **BQuMe⁺**, undergoing fluorophore quenching by PET. (d) Representation of changes in multi-state fluorescence: intramolecular PET quenching, fluorescence turn-on by single electron transfer (SET) with an amine, and collisional quenching with excess amine.

Sensing systems that display turn-off responses (Figure 1a) are common. They are easier to identify by simply screening a fluorescent compound against various stimuli for quenching. Sometimes, they may even self-identify by serendipity after exposure to a chemical agent. By contrast, the identification of a turn-on sensor is less straightforward. It could be pursued by screening every potential but non-fluorescent compound against various analytes of interest to find examples that turn on the fluorescence; not only must the potential sensor be sensitive to the analyte, but the product of the reaction also needs to be highly emissive. The ideal case, by contrast, is to program a mechanism into the sensor that will enable the fluorescence to be turned off, and then on again, in a controlled way. Fortunately, A. P. de Silva developed a general approach (Figure 1c) to create turn-on fluorescent molecular sensors,⁸ which he originally pioneered with cations.³⁴ Typically, a fluorophore is designed to be initially quenched by a preprogrammed photoinduced electron transfer (PET). Therefore, light absorption excites the fluorophore followed by PET to a covalently-linked acceptor and subsequent back electron transfer to reset the sensor. These electron transfer steps open up a non-radiative decay pathway to quench the fluorescence. Subsequent analyte binding or interaction with the electron acceptor inhibits the PET pathway to produce an analyte-dependent shut down of the non-radiative decay to turn on fluorescence. The essence of this approach is the combination of tunable electron-transfer processes with analyte interactions (Figure 1).

We saw an opportunity to implement these design principles with a 4,4-difluoro-4-bora-3a,4a-diaza-*s*-indacene (BODIPY) fluorophore. These dyes have garnered interest as one of the most versatile fluorescent sensors with high quantum yields and photostability.³⁵ These dyes are widely used as labeling agents,³⁶⁻³⁹ laser dyes,⁴⁰⁻⁴¹ and sensors.⁴²⁻⁴⁴ PET-quenched BODIPY dyes⁴⁵ have been used as turn-on sensors for a range of analytes, including anions (e.g., hypochlorite),⁴⁶

cations (e.g., zinc, magnesium, and H^+),⁴⁷⁻⁴⁹ and neutral compounds (e.g., cysteine, thiols, and phosgene).⁵⁰⁻⁵² We were drawn to previous work that showed the BODIPY's fluorescence could be quenched by PET using a covalently-linked methyl-pyridinium as electron acceptor.⁵³⁻⁵⁴ We originally set out to use this platform to create a turn-on fluorescent sensor for chloride. For this reason, we modified the original dye structure by replacing the methyl-pyridinium with methyl-quinolinium to utilize the latter's dose-dependent response to halides by collisional quenching.⁵⁵ Serendipitously, we identified that it was the amine impurities in our tetraethyl ammonium chloride salt⁵⁶ that produced the turn-on response we initially observed. Thus, we report here the design, discovery, properties, and the mechanism of behavior displayed by this new class of amine-sensitive quinolinium-BODIPY probe (Figure 1).

We describe the multi-state dose-response of a BODIPY-based probe. Multi-state sensing in this context is of a single BODIPY probe such that the fluorescence is modulated by three different processes. The sensor is dose-responsive as a result of switching between the two processes over different amine concentration ranges. Prior examples of dose-responsive sensors use two recognition sites to bind the analyte; for example using heteroditopic ligands for zinc sensing.⁵⁷⁻⁵⁹ The fluorescence of the described BODIPY probe is modulated by amine concentrations, but not by a discrete recognition site. First, the BODIPY fluorophore was preprogrammed to be quenched (turned off) by intramolecular PET to the methyl quinolinium acceptor (Figure 2a). We then discovered two concentration-dependent mechanisms by which the BODIPY fluorescence is modulated by amines (Figure 1d). The initial turn-on of fluorescence at lower amine concentration requires light irradiation and involves modulation of the PET from the BODIPY to the quinolinium. Specifically, single electron transfer (SET) from the amine to the BODIPY core and putative decomposition of the quinolinium radical shuts down the PET-based

non-radiative decay to turn on the fluorescence (Figure 2b). At higher concentrations of amine (50 mM – 1 M), we observed collisional quenching of the fluorescence. The balance of the preprogrammed quenching mechanism and the two amine sensing mechanisms results in a multi-state fluorescence response.

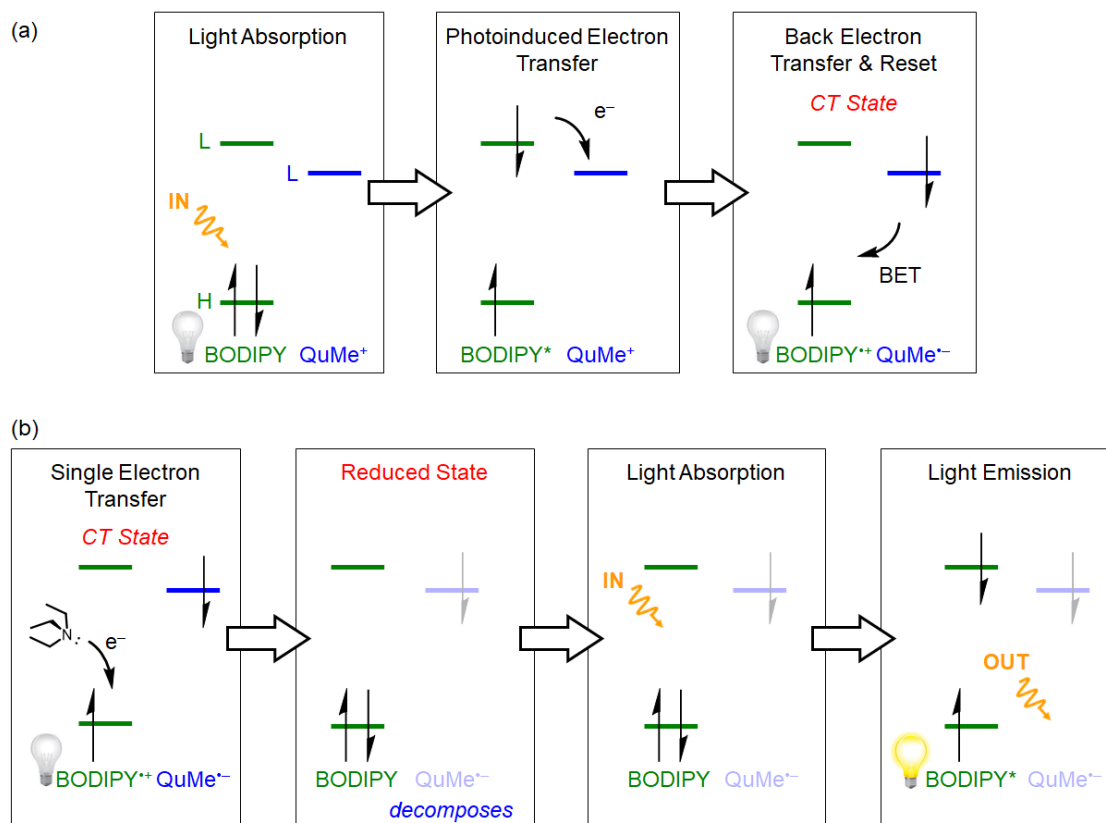


Figure 2. Hypothesized mechanisms of the first two modes of BODIPY fluorescence modulation.

(a) Fluorescence quenching by internal PET from the photoexcited BODIPY to the methyl-quinolinium and non-radiative back electron transfer (BET). (b) Fluorescence turn-on by single electron transfer (SET) from the amine to the charge-transfer excited state and decomposition of the methyl-quinolinium radical.

Results and Discussion:

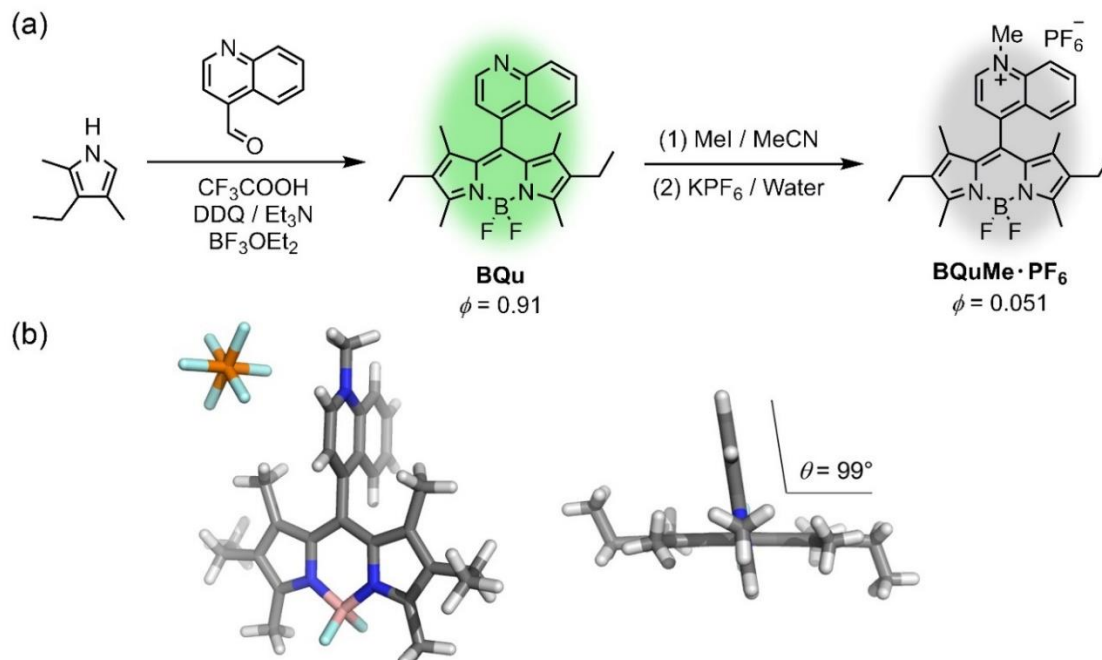


Figure 3. (a) Synthesis of the fluorescent control compound, **BQu**, and the probe, **BQuMe•PF₆**. (b) Crystal structure of **BQuMe•PF₆**.

The synthesis of the probe (**BQuMe⁺**, Figure 3a) involved the traditional one-pot preparation⁶⁰ of the BODIPY core by reaction of 3-ethyl-2,4-dimethylpyrrole with 4-quinolinecarboxaldehyde. As expected, the resulting intermediate, **BQu**, was highly emissive. This species served as an essential control compound for this study. Following methylation, the hexafluorophosphate (PF_6^-) salt was prepared by metathesis, as verified by ^{19}F NMR (Figure S29). A crystal structure of the probe, **BQuMe•PF₆**, (Figure 3b) shows the BODIPY and quinolinium moieties are orthogonal. Thus, the electron donor (BODIPY) and acceptor (methyl-quinolinium) moieties are likely to be poorly coupled, which is a typical requirement of PET. Here, the coupling is broken geometrically rather than by using a non-conjugated linker.

The control compound, **BQu**, was found to be highly fluorescent ($\phi = 0.91 \pm 0.02$, $\epsilon_{530} = 60,000 \text{ M}^{-1} \text{ cm}^{-1}$, $\tau = 7.12 \pm 0.03 \text{ ns}$, Figures S2 and S4). Upon methylation to the *N*-methyl quinolinium, **BQuMe⁺**, fluorescence was quenched ($\phi = 0.051 \pm 0.004$, $\epsilon_{530} = 14,000 \text{ M}^{-1} \text{ cm}^{-1}$, $\tau = 6.40 \pm 0.01 \text{ ns}$, Figures S3 and S4). These values are consistent with the changes seen previously as the pyridine analogue is methylated to the pyridinium, e.g., $\phi = 0.5$ drops to 0.03 and $\epsilon = 59,000$ to $26,000 \text{ M}^{-1} \text{ cm}^{-1}$, with quantum yields reduced by a factor of 17 and the molar absorptivity by two.⁵³

Assuming the quenching arises from a PET mechanism (Figure 2a), the probe is set up for a de Silva style mechanism of turn-on sensitivity with a complementary analyte disrupting the preprogrammed off state. After formation of the charge-transfer state by internal PET (Figure 2b), the amine undergoes a SET into the BODIPY core. The putative methyl-quinolinium radical that is produced appears to decompose. The net result of this process is removal of the PET quenching that reinstates BODIPY fluorescence (Figure 2b).

Starting from the initially dark form of the probe, **BQuMe⁺**, at a low concentration of 1 μM (acetonitrile, MeCN), we observed a turn-on response to 5 mM of triethylamine (TEA, Figure 4). We observed the turn-on response grow during constant light irradiation over the course of five hours (Figure 4a, Figure S6). Without the light irradiation, we did not observe any fluorescence turn-on with exposure to the amines in the dark over a two hour period (Figure S6). Consistent with our expectation (Figure 2b), the light dependence of the turn-on response indicated that the reaction between the amine and the probe is mediated by the probe's excited state.

In order to characterize the fully turned-on state of the probe, we added a large excess (5 mM) of TEA in solution (MeCN) to produce the on state of the probe. The result was a 190-fold increase in fluorescence intensity (Figure 4a) after five hours of light irradiation. The quantum

yield of the probe grew to 0.89 ± 0.10 , which is well within error of the quantum yield measured from the fluorescent control compound, **BQu**. This similarity implied that the PET quenching mechanism is fully shut down, completely restoring the BODIPY fluorescence to the entire sample in solution; quantitative conversion.

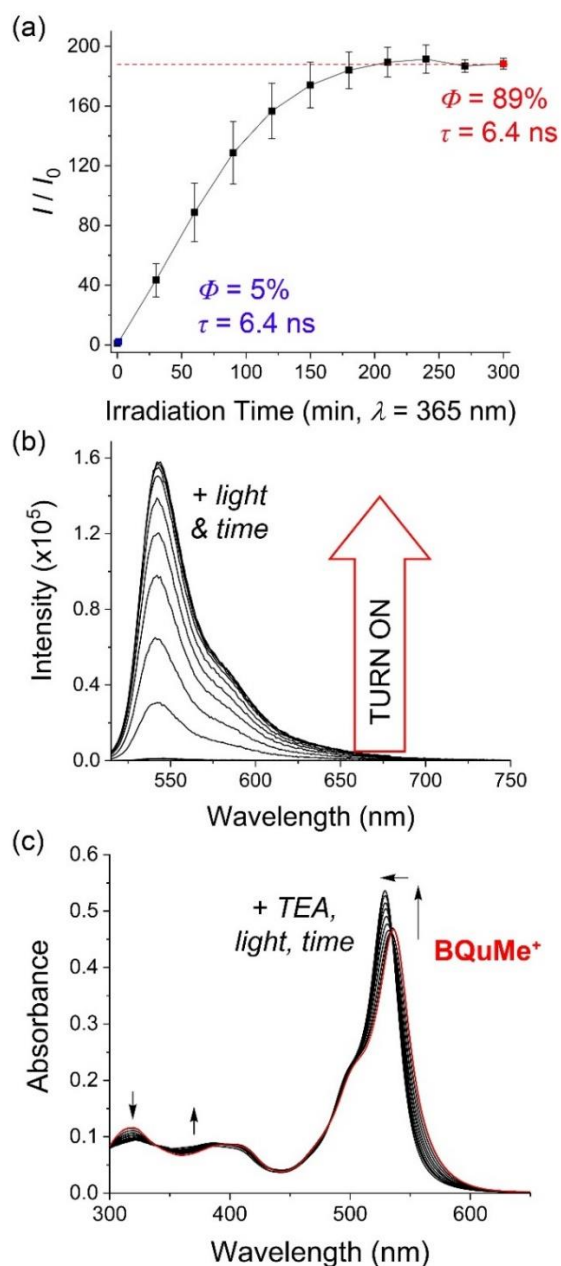


Figure 4. (a) The change in fluorescence over time of **BQuMe**⁺ (1 μ M, degassed with argon, MeCN, $\lambda_{\text{exc}} = 510$ nm) upon addition of 5 mM of triethylamine and UV irradiation. The quantum

yield and lifetime are highlighted for the probe alone (blue) and after being turned on (red). (b) Representative fluorescence emission spectra of **BQuMe⁺** (1 μ M, degassed with argon, MeCN, $\lambda_{\text{exc}} = 510$ nm) with triethylamine (5 mM) and UV irradiation ($\lambda = 365$ nm) increasing over five hours. (c) Absorption spectral changes of **BQuMe⁺** (10 μ M, MeCN) upon addition of TEA (5 mM) and UV light irradiation ($\lambda = 365$ nm) over the course of two hours.

We hypothesized that the amine reacted after formation of the charge-transfer state of the probe (Figure 2b) and examined the photophysical changes over the course of the reaction in order to further understand the reaction. We did not observe any significant changes in the spectral line shape of the emission spectrum during the turn on (Figure 4b). This finding suggested that the BODIPY core is not chemically modified by the amine but rather the reaction is ultimately perturbing the quinolinium ring system (Figure 2b). To examine the perturbation of the quinolinium, we monitored the reaction by absorption spectroscopy. Over the course of the turn-on period, we saw the absorption spectra of the probe, **BQuMe⁺**, shift over time to more closely resemble the spectral line shape observed for the fluorescent control compound, **BQu** (Figure 4c, Figure S7). We observed shifts in the characteristic BODIPY π - π^* transition at ~ 530 nm toward the peak maximum of the fluorescent control compound, **BQu** (Figure 4c). We also observed shifts away from the absorption peak assigned to the methyl-quinolinium at 317 nm (Figure 4c, Figure S7). Overall, the combination of the spectral shifts and quantum yield measurements provide evidence that, over the course of the reaction, the BODIPY core is no longer participating in PET to the quinolinium ring.

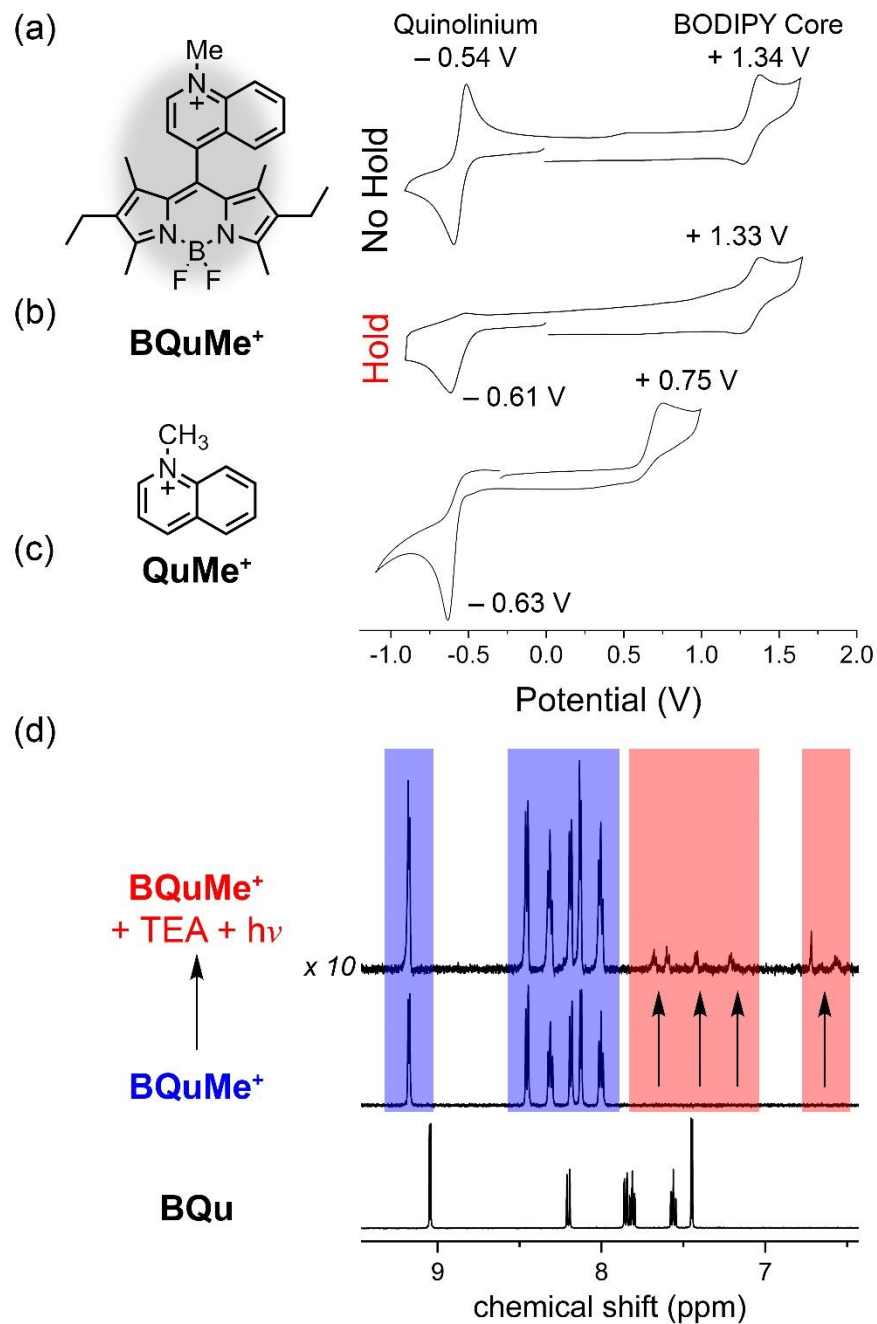


Figure 5. (a) Electrochemical analysis of **BQuMe⁺** (1 mM, MeCN, no amine present) by cyclic voltammetry and (b) with a 60 second hold at -1 V. (c) Cyclic voltammetry of methyl-quinolinium ring (**QuMe⁺**, 1 mM, MeCN). (d) Aromatic region of the ^1H NMR spectra of **BQuMe⁺** (5 mM, CD_3CN , degassed with argon) before and after adding triethylamine (100 mM) and UV irradiation ($\lambda = 365$ nm) for 90 minutes in comparison to **BQu** (5 mM).

We hypothesized that the photodriven reaction with amine chemically altered the quinolinium moiety to shut down the PET process of the parent **BQuMe**⁺ thereby restoring the fluorescence of the BODIPY core. If the amine is undergoing SET to the probe (Figure 2b), we hypothesized that we could model the product of the SET with the amine by using electrochemistry. That is, the photoproduct and electrochemically reduced states are both expected to be the same.

We compared the redox properties of the probe, **BQuMe**⁺, to that of methyl-quinolinium, **QuMe**⁺ (Figure 5). An irreversible one-electron reduction of methyl-quinolinium, **QuMe**⁺, occurred at -0.63 V (Figure 5c). Prior work shows the reduced methyl-quinolinium forms a radical and that the radical reversibly dimerizes at the carbon *para* to the ring's nitrogen.⁶¹ The authors proposed that it goes via a radical-mediated mechanism. Substitution at the carbon *para* to the nitrogen prevents dimerization.⁶¹ In our case, this *para* site is substituted by BODIPY and is expected to inhibit the reaction of the reduction product. Consistently, the redox properties of **BQuMe**⁺ shows the appearance of an electrochemically reversible one-electron reduction at -0.59 V to form a putative radical with its corresponding reoxidation at -0.50 V (Figure 5a). Only when we hold the potential at -1.0 V for 60 seconds do we provide more time for the reduced quinolinium to react as seen in the loss of the reoxidation peak (Figure 5b). The irreversible reduction of the quinolinium on the probe, **BQuMe**⁺, in the electrochemistry indicates that the reduction of the quinolinium upon photoreaction with the amine would also be irreversible.

Based on the electrochemistry, we aimed to characterize the possible photoproduct with ¹H NMR spectroscopy. To observe the photoproduct, we repeated the reaction using a significantly higher concentration of probe (5 mM) with excess amine (100 mM). The reaction was monitored over ninety minutes, during which time the sample was irradiated with light. The ¹H NMR

spectrum revealed new peaks growing in at lower chemical shifts (~ 7.5 ppm) than the aromatic peaks of the parent probe, consistent with a loss of aromaticity on the quinolinium rings (Figure 5d). The peaks corresponding to the BODIPY core were undisturbed by the reaction (Figure S8). The new ^1H NMR peaks did not align with the aromatic peaks of the fluorescent control compound, **BQu**, indicating the reaction was not a simple loss of the methyl group from the methyl-quinolinium ring (Figure 5d). In an effort to increase the product conversion, we increased the concentration of amine to 1 M relative to the 5 mM of probe in solution. However, the larger quantity of amine resulted in a third set of peaks appearing, indicating multiple decomposition products (Figure S10). The results of the NMR analysis are consistent with a photodriven reaction chemically modifying the methyl-quinolinium, likely a loss of aromaticity. The modified methyl-quinolinium is thus not able to participate in the PET quenching of the BODIPY.

We studied the concentration dependence of the turn-on response, expecting that the probe could be used as a traditional sensor. However, we saw a new process that also modulated the BODIPY fluorescence (Figure 6a). At low concentrations (e.g., 1 mM), we observed the expected linear turn-on response with light exposure for two hours. At high concentrations (>10 mM), the linear portion of the turn-on response showed a saturation with just 15 minutes of light irradiation. Surprisingly, the saturation level decreased as we raised the concentration of amine. The decrease in fluorescence with higher amine concentrations implied that a quenching mechanism was activated.

Based on the structural similarities between the probe, **BQuMe⁺**, and the fluorescent control compound, **BQu**, we hypothesized that the quenching mechanisms of the two compounds would be the same at high amine concentrations. To test this idea, we conducted a Stern-Volmer analysis by titrating amine into a solution of the fluorescent control compound, **BQu**. Consistent

with previous literature on other dye classes, e.g., coumarin and styryl pyridine,^{17,21} we observed quenching of the fluorescent control compound, **BQu**, with increasing concentration of amine in solution (Figure 6b, Figure S17). Our analysis with **BQu** provided a Stern-Volmer quenching constant of $20.6 \pm 0.2 \text{ M}^{-1}$ and a corresponding bimolecular rate constant of $2.9 \pm 0.1 \times 10^9 \text{ M}^{-1} \text{ s}^{-1}$ (Equation S2). The changes in the fluorescence lifetime of **BQu** upon addition of amine (Figure S17) were consistent with collisional quenching.²⁸ As expected, the quenching of **BQu** was observed over the same concentration range as the plateau seen with **BQuMe**⁺.

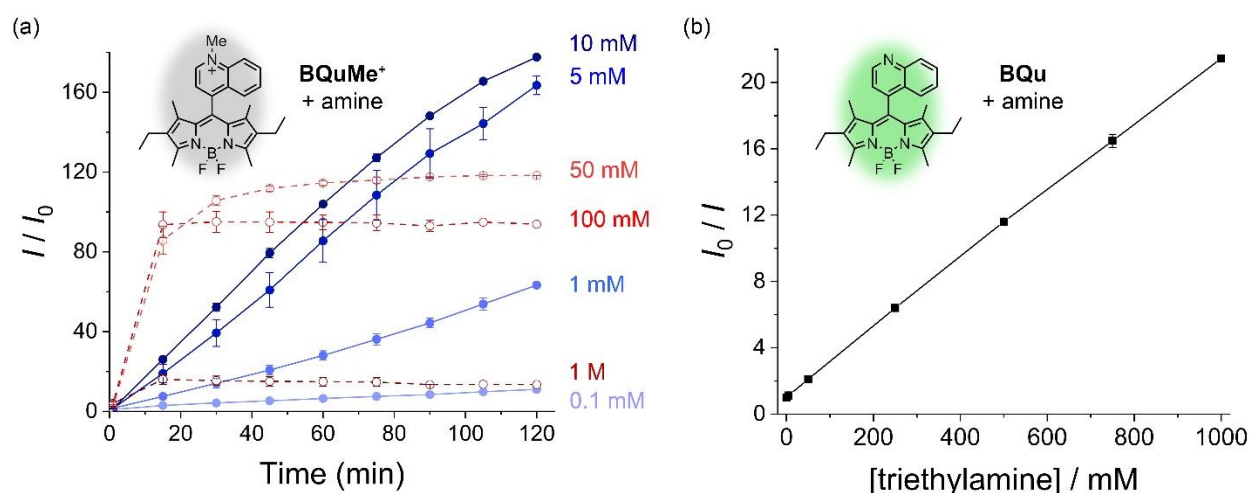


Figure 6. (a) Fluorescence response of **BQuMe**⁺ (1 μM , MeCN, $\lambda_{\text{exc}} = 510 \text{ nm}$) with addition of various concentrations of triethylamine (UV-irradiation with $\lambda = 365 \text{ nm}$ between time points, under argon). (b) Stern-Volmer plot showing the fluorescence quenching of the control compound, **BQu** (1 μM , MeCN), in the presence of triethylamine.

In order to analyze the plateau response of **BQuMe**⁺, we plotted the concentration (0.05, 0.1, and 1 M) versus the average intensity loss (I_0 / I) after the intensity had stabilized (>45 minutes). A Stern-Volmer analysis of the data generated an apparent diffusion-limited rate constant ($1.7 \pm 0.1 \times 10^9 \text{ M}^{-1} \text{ s}^{-1}$, Figure S18). The similarity in the quenching rate constants

between the two compounds over the same concentration regime implied the same collisional quenching mechanism was operating.

Overall, the **BQuMe⁺** probe has two amine sensing mechanisms. The linear turn-on response with time occurs at the low amine concentrations while a plateau response is present at high amine concentrations. The fluorescence is turned on at low concentrations of amine (0.1 – 10 mM) by SET from the amine to the BODIPY core of the charge-transfer state (Figure 2b) generating an emissive photoproduct. The initial photoproduct is believed to be the reduced state of the methyl-quinolinium, which decomposes into a non-aromatic heterocycle. At higher amine concentrations (≥ 50 mM), we also observed bimolecular collisional quenching to become an active process. The collisional quenching modulates the fluorescence response of **BQuMe⁺** across the same concentration range as the amine quenches the fluorescence of **BQu**. At the higher concentrations, the rate of SET and the subsequent irreversible decomposition to the on-state of the probe are hypothesized to occur to a substantial extent. It is then the collisional quenching of this on state that generates the initially high plateau at the mid-range (50 mM) concentrations, which decreases in intensity as amine concentrations are raised.

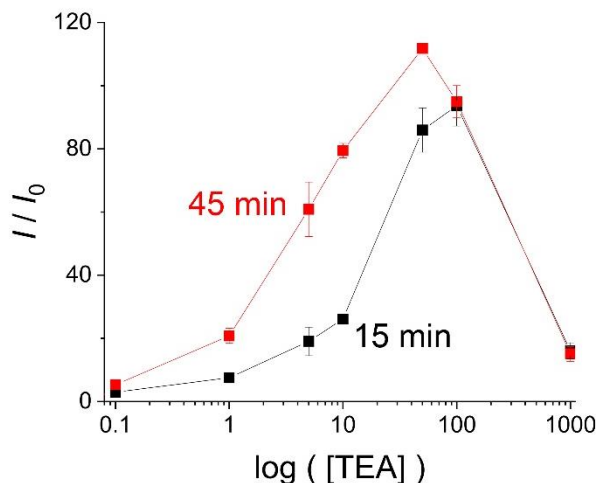


Figure 7. Stern-Volmer calibration curve for amine sensing with the probe. Fluorescence emission turn-on response of **BQuMe⁺** (1 μ M, MeCN, degassed with argon) after addition of triethylamine at two time points of UV irradiation ($\lambda = 365$ nm, black = 15 minutes, red = 45 minutes).

The multi-state sensitivity to amine concentration has the potential to be used for sensing. The sensor can be used directly to detect amines up to 50 mM. If the dynamic range needs to be extended further, however, a different approach is needed. Comparing the fluorescence intensity change at two time points of UV-irradiation (Figure 7) allows for discrimination of high amine concentrations. For example, a 15-minute measurement (black trace) of the intensity turn-on (I/I_0) of 15 could correspond to either 5 mM or 1 M of amine. Differentiation between the two concentrations could be made after further light exposure. The 5 mM amine sample would grow in fluorescence intensity while the latter would remain constant.

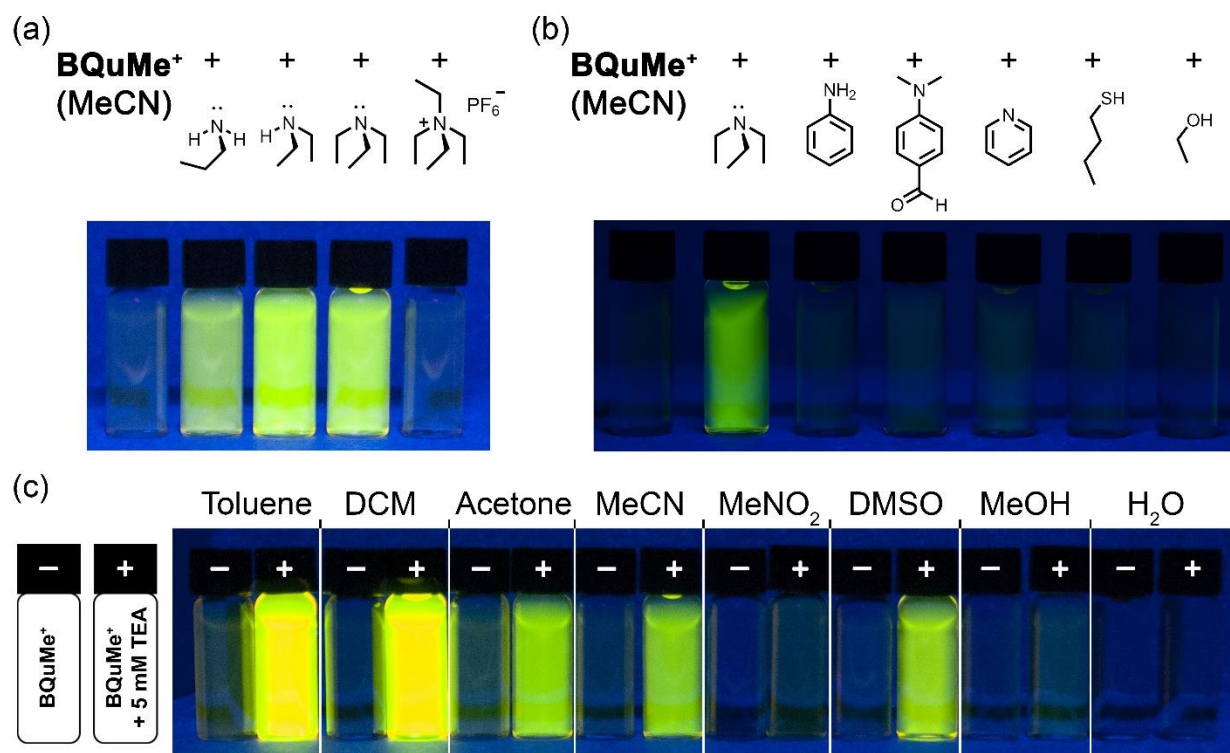


Figure 8. (a) Turn-on response of **BQuMe**⁺ (10 μM, MeCN) in the presence of various aliphatic amines (5 mM) after two hours of UV irradiation (λ = 365 nm). (b) Selectivity screen of **BQuMe**⁺ (10 μM, MeCN) against triethylamine, aniline, *p*-(dimethylamino)benzaldehyde, pyridine, 1-butanethiol, and ethanol (5 mM) after two hours of UV irradiation (λ = 365 nm). (c) Solvent dependent turn-on response of **BQuMe**⁺ (10 μM) with trimethylamine (5 mM) after two hours of UV irradiation (λ = 365 nm).

We tested the generality of the turn-on response to amines by reacting the probe, **BQuMe**⁺, with a range of amines in different solvents (Figure 8). All of the aliphatic amines tested resulted in a turn-on response. As expected, quaternary ammonium groups had no impact on the fluorescence, consistent with the involvement of the amine's lone-pair in the observed reaction-based sensing mechanism (Figure 8a). Aromatic amines, aliphatic thiols, and aliphatic alcohols did not result in a turn-on response (Figure 8b). We see that the formation of the quenched charge-

transfer state (Figure 2b) was not affected by solvent polarity on account of the fact that the probe remained initially quenched in all the solvents we examined (Figure 8c). We observe that the turn-on response to the amine changes with a solvent and hypothesize that it reflects the solvent's hydrogen bond donating ability.⁶² Non-protic solvents (toluene, dichloromethane, acetone) facilitated the turn-on response, while polar protic solvents (water, methanol) inhibited the change in fluorescence (Figure 8c).

To better understand how methylation of the quinoline moiety leads to the photophysical changes, we conducted density functional theory (DFT) calculations of the frontier molecular orbitals. In the fluorescent control compound, **BQu**, both the HOMO and LUMO are localized on the BODIPY core (Figure 9a), which is consistent with the orthogonal arrangement of the quinoline having a negligible effect on fluorescence. The LUMO+1 is localized on the quinoline. Methylation to **BQuMe⁺** leads to dramatic stabilization of the quinolinium-localized orbital by 1.5 eV leading to a re-ordering such that it becomes the LUMO (Figure 9b).

The impact of the orbital re-ordering upon methylation was examined using time-dependent DFT (TDDFT) calculations. Upon methylation, we see a change in character of the lowest energy $S_1 \rightarrow S_0$ transition from highly allowed ($f = 0.78$) $\pi\pi$ for **BQu** to charge transfer for **BQuMe⁺** with a lower oscillator strength ($f = 0.03$), supporting the experimentally-observed quenching. Consistently, other works^{54, 63-64} have also suggested that charge transfer states in BODIPY-containing chromophores undergo rapid de-excitation by intersystem crossing to non-emissive triplet states. The low oscillator strength of the charge transfer state is also consistent with the suggested PET mechanism, while the absorption spectrum is dominated by the BODIPY band for both the fluorescent control compound, **BQu**, and the probe, **BQuMe⁺**.

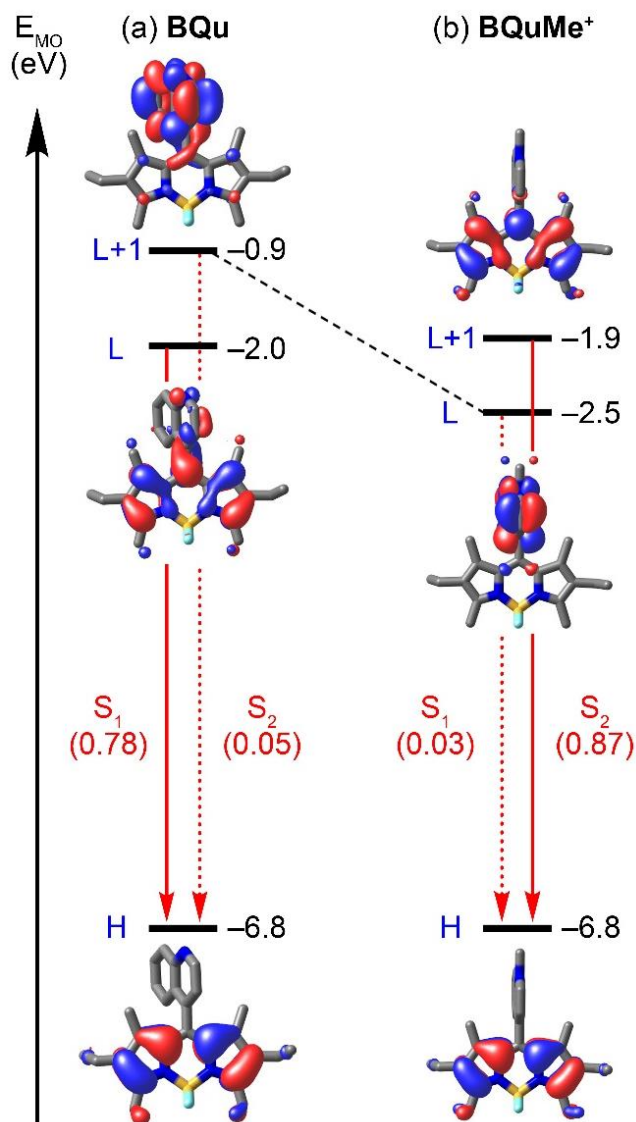


Figure 9. Vertical transitions calculated using TDDFT for the emissions of (a) **BQu** and (b) **BQuMe⁺** including solvation effects (acetonitrile). All vertical transitions were dominated by a single electronic transition (Tables S2 and S3). The orbitals shown are from natural transition orbital analysis. Oscillator strengths (f) for the electronic transitions are included in parentheses; solid lines indicate higher oscillator strengths and dashed lines indicate lower oscillator strengths.

Conclusion

We discovered a multi-state and dose-dependent response of a BODIPY-based fluorophore towards amines. The multi-state character is based on three processes that modulate the BODIPY fluorescence. First, the fluorescence is preprogrammed to be quenched by internal PET to a quinolinium ring system. Second, fluorescence is restored by SET from the amine analyte to the photoexcited BODIPY core generating a photoproduct such that the internal PET quenching mechanism no longer operates. Third, at high concentrations of amine, we observed collisional fluorescence quenching of the native BODIPY core. The non-methylated **BQu** compound only displays the high-concentration collisional quenching thereby verifying the role of internal PET within **BQuMe⁺** for generating the multi-state response to amines. The probe is able to determine amine concentrations over a 10^{-4} – 10^1 M dynamic range by comparing the fluorescence response at two time points. The three processes combine together to modulate the BODIPY fluorescence, cumulating in the first example of multi-state amine sensing.

ASSOCIATED CONTENT

Supporting Information is available on the journal website: full experimental details, Figures S1-S34, and Tables S1-S4 (PDF), pdb files for computed structures, and the crystal structure of **BQuMe•PF₆** (CIF).

AUTHOR INFORMATION

Corresponding Author

*aflood@indiana.edu

Conflicts of interest

There are no conflicts of interest to declare.

ACKNOWLEDGMENT

This work was supported by the Chemical Sciences, Geosciences, and Biosciences Division of the Basic Energy Sciences Program of the US Department of Energy Office of Science (DE-FG02-09ER16068). AHF and KLV also acknowledge support from the Luther Dana Waterman Professorship. AHF and SEC acknowledge support from the TUBITAK 2214-A fellowship. AHF acknowledges early support by the Office of the Vice Provost for Research, Indiana University with their Faculty Research Support Program. A.H.F and K.L.V thank Dr. Irina Tsvetkova for assistance with the fluorescence experiments, and Dr. Jonathan A. Karty from the Indiana University Mass Spectrometry Facility for support.

REFERENCES

1. Biji, K. B.; Ravishankar, C. N.; Venkateswarlu, R.; Mohan, C. O.; Gopal, T. K. S., *J. Food Sci. Tech.*, **2016**, *53*, 2210-2218.
2. Erdag, D.; Merhan, O.; Yildiz, B., *Biochemical and Pharmacological Properties of Biogenic Amines, Biogenic Amines*. IntechOpen: 2018.
3. Neurath, G. B.; Dünker, M.; Pein, F. G.; Ambrosius, D.; Schreiber, O., *Food Cosmet. Toxicol.*, **1977**, *15*, 275-282.
4. Stavric, B., *Food Chem. Toxicol.*, **1994**, *32*, 977-994.
5. Pinheiro, H. M.; Touraud, E.; Thomas, O., *Dyes Pigments*, **2004**, *61*, 121-139.
6. Popli, S.; Patel, U. D., *Int. J. Environ. Sci. Tech.*, **2015**, *12*, 405-420.

7. Wu, D.; Sedgwick, A. C.; Gunnlaugsson, T.; Akkaya, E. U.; Yoon, J.; James, T. D., *Chem. Soc. Rev.*, **2017**, *46*, 7105-7123.
8. Daly, B.; Ling, J.; de Silva, A. P., *Chem. Soc. Rev.*, **2015**, *44*, 4203-4211.
9. Udenfriend, S.; Stein, S.; Böhlen, P.; Dairman, W.; Leimgruber, W.; Weigele, M., *Science*, **1972**, *178*, 871-872.
10. Chaicham, A.; Sahasithiwat, S.; Tuntulani, T.; Tomapatnanaget, B., *Chem. Commun.*, **2013**, *49*, 9287-9289.
11. Fu, Y.; He, Q.; Zhu, D.; Wang, Y.; Gao, Y.; Cao, H.; Cheng, J., *Chem. Commun.*, **2013**, *49*, 11266-11268.
12. Lee, M. H.; Yoon, B.; Kim, J. S.; Sessler, J. L., *Chem. Sci.*, **2013**, *4*, 4121-4126.
13. Shcherbakova, E. G.; Minami, T.; Brega, V.; James, T. D.; Anzenbacher Jr., P., *Angew. Chem. Int. Edit.*, **2015**, *54*, 7130-7133.
14. Sathiskumar, U.; Easwaramoorthi, S., *ChemistrySelect*, **2019**, *4*, 7486-7494.
15. Pushina, M.; Farshbaf, S.; Shcherbakova, E. G.; Anzenbacher, P., *Chem. Commun.*, **2019**, *55*, 4495-4498.
16. Jia, R.; Tian, W.; Bai, H.; Zhang, J.; Wang, S.; Zhang, J., *Nat. Commun.*, **2019**, *10*, 795.
17. Nad, S.; Pal, H., *J. Phys. Chem. A*, **2000**, *104*, 673-680.
18. Broglia, M. F.; Bertolotti, S. G.; Previtali, C. M., *Photochem. Photobiol.*, **2007**, *83*, 535-541.
19. Huang, L.; Zhao, J., *RSC. Adv.*, **2013**, *3*, 23377-23388.
20. Luo, G.-G.; Fang, K.; Wu, J.-H.; Dai, J.-C.; Zhao, Q.-H., *Phys. Chem. Chem. Phys.*, **2014**, *16*, 23884-23894.
21. Asha Jhonsi, M.; Kathiravan, A., *J. Lumin.*, **2014**, *145*, 188-193.

22. Sriramulu, D.; Valiyaveetil, S., *Dyes Pigments*, **2016**, *134*, 306-314.
23. Hu, Y.; Ma, X.; Zhang, Y.; Che, Y.; Zhao, J., *ACS Sensors*, **2016**, *1*, 22-25.
24. Pellegrin, Y.; Odobel, F., *C. R. Chim.*, **2017**, *20*, 283-295.
25. Venkatesh, Y.; Munisamy, V.; Ramakrishna, B.; Kumar, P. H.; Mandal, H.; Bangal, P. R., *Phys. Chem. Chem. Phys.*, **2017**, *19*, 5658-5673.
26. Zhai, L.; Shu, Y.; Sun, J.; Sun, M.; Song, Y.; Lu, R., *Eur. J. Org. Chem.*, **2019**, *2019*, 3093-3100.
27. Venkatesan, M.; Mandal, H.; Bheerappagari, R.; Bangal, P. R., *J. Photoch. Photobiol. A.*, **2019**, *376*, 212-223.
28. Lakowicz, J. R., *Topics in fluorescence spectroscopy*. Plenum Press: New York, 1994; Vol. 4.
29. He, C.; He, Q.; Deng, C.; Shi, L.; Zhu, D.; Fu, Y.; Cao, H.; Cheng, J., *Chem. Commun.*, **2010**, *46*, 7536-7538.
30. Fu, Y.; Shi, L.; Zhu, D.; He, C.; Wen, D.; He, Q.; Cao, H.; Cheng, J., *Sensor Actuat. B-Chem.*, **2013**, *180*, 2-7.
31. Dong, L.; Deng, C.; He, C.; Shi, L.; Fu, Y.; Zhu, D.; Cao, H.; He, Q.; Cheng, J., *Sensor Actuat. B-Chem.*, **2013**, *180*, 28-34.
32. Sandeep, A.; Praveen, V. K.; Kartha, K. K.; Karunakaran, V.; Ajayaghosh, A., *Chem. Sci.*, **2016**, *7*, 4460-4467.
33. Mani, P.; Ojha, A. A.; Reddy, V. S.; Mandal, S., *Inorg. Chem.*, **2017**, *56*, 6772-6775.
34. de Silva, A. P.; de Silva, S. A., *J. Chem. Soc. Chem. Commun.*, **1986**, 1709-1710.
35. Bañuelos, J., *Chem. Rec.*, **2016**, *16*, 335-348.
36. Li, L.; Han, J.; Nguyen, B.; Burgess, K., *J. Org. Chem.*, **2008**, *73*, 1963-1970.

37. Niu, S. L.; Ulrich, G.; Ziessel, R.; Kiss, A.; Renard, P.-Y.; Romieu, A., *Org. Lett.*, **2009**, *11*, 2049-2052.
38. Niu, S. L.; Massif, C.; Ulrich, G.; Ziessel, R.; Renard, P.-Y.; Romieu, A., *Org. Biomol. Chem.*, **2011**, *9*, 66-69.
39. Ono, M.; Watanabe, H.; Ikehata, Y.; Ding, N.; Yoshimura, M.; Sano, K.; Saji, H., *Sci. Rep.*, **2017**, *7*, 3337.
40. Mula, S.; Ray, A. K.; Banerjee, M.; Chaudhuri, T.; Dasgupta, K.; Chattopadhyay, S., *J. Org. Chem.*, **2008**, *73*, 2146-2154.
41. Bañuelos, J.; Martín, V.; Gómez-Durán, C. F. A.; Córdoba, I. J. A.; Peña-Cabrera, E.; García-Moreno, I.; Costela, Á.; Pérez-Ojeda, M. E.; Arbeloa, T.; Arbeloa, Í. L., *Chem. Eur. J.*, **2011**, *17*, 7261-7270.
42. Baruah, M.; Qin, W.; Vallée, R. A. L.; Beljonne, D.; Rohand, T.; Dehaen, W.; Boens, N., *Org. Lett.*, **2005**, *7*, 4377-4380.
43. Peng, X.; Du, J.; Fan, J.; Wang, J.; Wu, Y.; Zhao, J.; Sun, S.; Xu, T., *J. Am. Chem. Soc.*, **2007**, *129*, 1500-1501.
44. Niu, L.-Y.; Guan, Y.-S.; Chen, Y.-Z.; Wu, L.-Z.; Tung, C.-H.; Yang, Q.-Z., *J. Am. Chem. Soc.*, **2012**, *134*, 18928-18931.
45. Lincoln, R.; Greene, L. E.; Krumova, K.; Ding, Z.; Cosa, G., *J. Phys. Chem. A*, **2014**, *118*, 10622-10630.
46. Shi, W.-J.; Huang, Y.; Liu, W.; Xu, D.; Chen, S.-T.; Liu, F.; Hu, J.; Zheng, L.; Chen, K., *Dyes Pigments*, **2019**, *170*, 107566.
47. Atilgan, S.; Ozdemir, T.; Akkaya, E. U., *Org. Lett.*, **2008**, *10*, 4065-4067.
48. Lin, Q.; Gruskos, J. J.; Buccella, D., *Org. Biomol. Chem.*, **2016**, *14*, 11381-11388.

49. Prasannan, D.; Arunkumar, C., *New J. Chem.*, **2018**, *42*, 3473-3482.
50. Wu, Q.; Zhou, J.; Wu, Y.; Yu, C.; Hao, E.; Jiao, L., *New J. Chem.*, **2016**, *40*, 1387-1395.
51. Kolemen, S.; Akkaya, E. U., *Coordin. Chem. Rev.*, **2018**, *354*, 121-134.
52. Kim, T.-I.; Kim, D.; Bouffard, J.; Kim, Y., *Sensor Actuat. B-Chem.*, **2019**, *283*, 458-462.
53. Ulrich, G.; Ziessel, R., *J. Org. Chem.*, **2004**, *69*, 2070-2083.
54. Harriman, A.; J Mallon, L.; Ulrich, G.; Ziessel, R., *Chem. Phys. Chem.*, **2007**, *8*, 1207-14.
55. Jayaraman, S.; Verkman, A. S., *Biophys. Chem.*, **2000**, *85*, 49-57.
56. Zucker, R. S., *Brain Research*, **1981**, *208*, 473-478.
57. Zhang, L.; Clark, R. J.; Zhu, L., *Chem. Eur. J.*, **2008**, *14*, 2894-2903.
58. Zhu, L.; Zhang, L.; Younes, A. H., *Supramol. Chem.*, **2009**, *21*, 268-283.
59. Kuang, G.-C.; Allen, J. R.; Baird, M. A.; Nguyen, B. T.; Zhang, L.; Morgan, T. J.; Levenson, C. W.; Davidson, M. W.; Zhu, L., *Inorg. Chem.*, **2011**, *50*, 10493-10504.
60. Loudet, A.; Burgess, K., *Chem. Rev.*, **2007**, *107*, 4891-4932.
61. Teplý, F.; Čížková, M.; Slavíček, P.; Kolivoška, V.; Tarábek, J.; Hromadová, M.; Pospíšil, L., *J. Phys. Chem. C*, **2012**, *116*, 3779-3786.
62. Marcus, Y., *Chem. Soc. Rev.*, **1993**, *22*, 409-416.
63. Qin, W.; Baruah, M.; Van der Auweraer, M.; De Schryver, F. C.; Boens, N., *J. Phys. Chem. A*, **2005**, *109*, 7371-7384.
64. Zhao, J.; Xu, K.; Yang, W.; Wang, Z.; Zhong, F., *Chem. Soc. Rev.*, **2015**, *44*, 8904-8939.